Boundary Observer for Output-Feedback Stabilization of Thermal-Fluid Convection Loop

Rafael Vazquez, *Member, IEEE*, and Miroslav Krstic, *Fellow, IEEE*

***Abstract*—In this paper, we consider a 2-D model of thermal fluid convection that exhibits the prototypical Rayleigh–Bernard convective instability. The fluid is enclosed between two cylinders, heated from above, and cooled from below, which makes its motion unstable for a large enough Rayleigh number. We design an stabilizing output feedback boundary control law for a realistic collocated setup, with actuation and measurements located at the outer boundary. Actuation is through rotation (direct velocity actuation) and heat flux (heating or cooling) of the outer cylinder, while measurements of friction and temperature are obtained at the same boundary. Though only a linearized version of the plant is considered in the design, an extensive closed loop simulation study of the nonlinear model shows that our design works for reasonably large initial conditions. A highly accurate approximation to the control kernels and observer output injection gains is found in closed form.**

***Index Terms*—Backstepping, boundary control, distributed parameter systems, flow control, partial differential equations (PDEs), observers, singularly perturbed systems, stabilization.**

I. Introduction

RECENT years have been marked by dramatic advances in active flow control; see for instance the survey [4] and references therein. Many particular problems have been considered, like vortex shedding [1], [12], turbulent channel flow control [3], [8], [16], or separation control [2]. However, the area of fluids subject to thermal gradients, despite its obvious practical engineering interest, has been mostly neglected.

In this paper, we consider a 2-D model of thermal fluid convection that exhibits the prototypical Rayleigh–Bernard convective instability [9]. The fluid is enclosed between two cylinders, heated from above and cooled from below. Imposing a temperature gradient induces density differences, which creates a circular motion that is opposed by viscosity and thermal diffusivity. For a large enough Rayleigh number, which is a function of physical constants of the system, geometry and temperature difference between the top and the bottom, the plant develops an instability.

The model was first formulated by Burns *et al.* [6], who solved the problem using a linear quadratic Gaussian (LQG) controller; the resulting Riccati equations were solved using a finite element method. Other efforts include a nonlinear backstepping design for a discretized version of the plant [5], but the result did not hold in the limit when the discrete grid approached the continuous, real domain. The design we present here is based on our previous work [16], where we designed a (full-state) control law to stabilize the linearized system based on singular perturbation analysis and nondiscretized partial differential equation (PDE) backstepping control. The control law we obtained was explicit and the design was done for the infinite dimensional continuous model.

We design an output feedback controller that uses the same controller as in [16], but uses an observer to obtain temperature estimates for the control law. The observer is designed using singular perturbations and the dual PDE backstepping observer design method [15]; this allows us to obtain readily implementable explicit observer gains.

The main ingredients of our design are singular perturbation theory and the backstepping method for infinite dimensional linear systems. Singular perturbation theory is a mature area [10] with a wealth of control applications, while backstepping is still recent [14], [15] but has already found application in flow control [1], [18], [19]. Combining both methods it is possible to design an output feedback control law which stabilizes the closed loop system; this is proved for a large enough Prandtl number, which is the ratio between kinematic viscosity and thermal diffusivity. In this problem, the inverse of the Prandtl number plays the role of the singular perturbation parameter.

We start this paper stating the mathematical model of the convection loop (see Section II) and transforming it into a suitable form for application of singular perturbation methods. In Section III, we show that the temperature can be decomposed into two new independent variables; we use this to express the system as the combination of two separate subsystem. The first of them is analyzed in Section IV, and stabilized with an output feedback controller designed by a Lyapunov method. Section V is concerned with the second subsystem and it is divided in several subsections. First a full state controller is designed, as in [16], using singular perturbation theory and a backstepping design. Then, using dual methods, an observer is designed and combined with the controller to obtain output feedback laws. Both the control and output injection kernels are found solving a linear hyperbolic PDE, which can be done numerically or symbolically. A highly accurate approximation to the kernels is found in closed form. We finish the section with a stability result based on both singular perturbation and backstepping theory. In Section VI, we present the output feedback controller for the entire system and state the main result of this paper. The

Manuscript received October 26, 2006. Manuscript received in final form June 26, 2008. First published August 18, 2009; current version published June 23, 2010. Recommended by Associate Editor C. Wang. This work was supported by NSF Grant CMS-0329662.

R. Vazquez is with the Departamento de Ingeniería Aeroespacial, Universidad de Sevilla, 41092 Seville, Spain (e-mail: rvazquez1@us.es).

M. Krstic is with the Department of Mechanical and Aerospace Engineering, University of California at San Diego, La Jolla, CA 92093-0411 USA (e-mail: krstic@ucsd.edu).

Digital Object Identifier 10.1109/TCST.2009.2028549

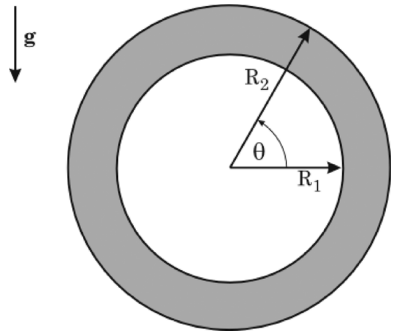

Fig. 1. Convection loop geometry.

theoretical result is supported by a numerical study, presented in Section VII, in which closed-loop simulations of the plant and control effort are shown. In these simulations the Rayleigh number is large enough for the plant to go open loop unstable, but the controller is able to overcome the instability. We finish with some concluding remarks in Section VIII. We also include the Appendix proving some technical results used through this paper.

II. Problem Statement

The geometry of the problem is shown in Fig. 1, and consists of fluid confined between two concentric cylinders of radius R_1 and R_2. The cylinders stand in a vertical plane, so that gravity acts as in Fig. 1. Under the assumption that the gap between the cylinders is small compared to the radius of the cylinders, i.e., $R_2 - R_1 \ll R_1 < R_2$, and using the Boussinesq approximation, the following non-dimensional model is derived (see [16] for details)

$$v_t = \frac{1}{\pi} P R_a C \int_0^{2\pi} \tau(t,r,\phi)\cos\phi d\phi + P\left(-\frac{v}{r^2} + \frac{v_r}{r} + v_{rr}\right) \quad (1)$$

$$\tau_t = \frac{d\pi}{2(R_1+R_2)} v\cos\theta - \frac{v}{r}\tau_\theta + \frac{\tau_{\theta\theta}}{r^2} + \frac{\tau_r}{r} + \tau_{rr} \quad (2)$$

where $v(t,r)$ is the azimuthal velocity (the radial velocity is neglected under the assumptions), $\tau(t,r,\theta)$ is the perturbation temperature about the equilibrium profile, and R_a and P are, respectively, the Rayleigh and Prandtl numbers. The boundary conditions are

$$v(t,R_1) = 0 \quad (3)$$

$$v(t,R_2) = V(t) \quad (4)$$

$$\tau_r(t,R_1,\theta) = 0 \quad (5)$$

$$\tau_r(t,R_2,\theta) = \Gamma(t,\theta) \quad (6)$$

where V and Γ are, respectively, the non-dimensional velocity and temperature control. Note that for a given time V is an scalar, while Γ is a function of the angle, as illustrated by Fig. 2. We also assume that measurements of $v_r(t,r)$ (proportional to skin friction) and $\tau(t,r,\theta)$ are available only for $r = R_2$.

Following the lines of the stability study of these equations in [5], the value of C in (1) is set so the system is stable for Rayleigh numbers less than unity and unstable otherwise.

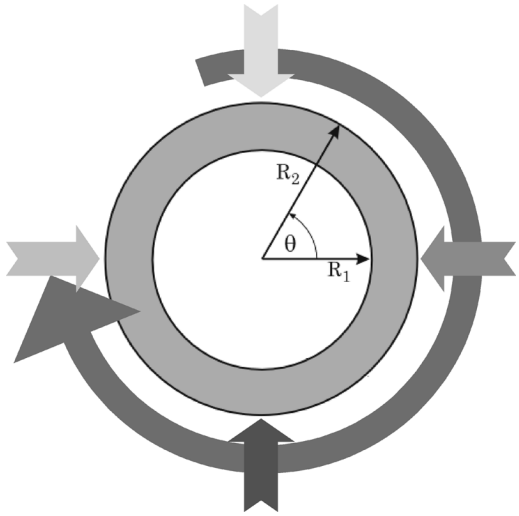

Fig. 2. Velocity and thermal actuation on the outer boundary of the convection loop. Measurements are obtained from the same boundary.

Defining $\epsilon = P^{-1}$, $A_1 = R_a C$, $A_2 = d\pi/2(R_1+R_2)$, dropping time dependence, and neglecting the nonlinear term, the linearized plant equations are the following:

$$\epsilon v_t = A_1 \frac{1}{\pi}\int_0^{2\pi} \tau(r,\phi)\cos\phi d\phi - \frac{v}{r^2} + \frac{v_r}{r} + v_{rr} \quad (7)$$

$$\tau_t = A_2 v\cos\theta + \frac{\tau_{\theta\theta}}{r^2} + \frac{\tau_r}{r} + \tau_{rr} \quad (8)$$

with the same boundary conditions (3)–(6).

We will design an output feedback control law to stabilize the linearized plant around the origin, therefore stabilizing—at least locally—the full nonlinear plant.

III. System Decomposition

Defining new variables

$$u(t,r) = \frac{1}{\pi}\int_0^{2\pi} \tau(t,r,\theta)\cos\theta d\theta \quad (9)$$

$$U(t) = \frac{1}{\pi}\int_0^{2\pi} \Gamma(t,\theta) d\theta \quad (10)$$

and letting $\zeta = \tau - u\cos\theta$ and $\Upsilon = \Gamma - U\cos\theta$, we can write the plant in (v,u,ζ) variables as

$$\epsilon v_t = A_1 u - \frac{v}{r^2} + \frac{v_r}{r} + v_{rr} \quad (11)$$

$$u_t = A_2 v - \frac{u}{r^2} + \frac{u_r}{r} + u_{rr}, \quad (12)$$

$$\zeta_t = \frac{\zeta_{\theta\theta}}{r^2} + \frac{\zeta_r}{r} + \zeta_{rr} \quad (13)$$

with boundary conditions

$$v(t,R_1) = 0, \quad v(t,R_2) = V(t) \quad (14)$$

$$u_r(t,R_1) = 0, \quad u_r(t,R_2) = U(t) \quad (15)$$

$$\zeta_r(t,R_1,\theta) = 0, \quad \zeta_r(t,R_2,\theta) = \Upsilon(t). \quad (16)$$

Remark 1: The variable u is the first cosine coefficient of the Fourier series of the periodic variable τ whereas ζ contains the remaining periodic components. The variable ζ verifies

$$\int_0^{2\pi} \zeta \cos\theta d\theta = \int_0^{2\pi} \tau \cos\theta d\theta - \pi u = 0 \tag{17}$$

and therefore is orthogonal (in the $L^2(0,2\pi)$ sense) to $u\cos\theta$. Hence, both u and ζ are independent and needed to recover τ.

Our design task is to find output feedback control laws Υ, V, and U such that the equilibrium profile $\zeta \equiv v \equiv u \equiv 0$ is exponentially stable. For the statement of stability, we define the norms

$$\|f\|^2_{L^2_\theta} = \int_0^{2\pi}\int_{R_1}^{R_2} f(r,\theta)^2 r dr d\theta \tag{18}$$

$$\|f\|^2_{H^1_\theta} = \|f\|^2_{L^2_\theta} + \|f_r\|^2_{L^2_\theta} + \|\frac{f_\theta}{r}\|^2_{L^2_\theta} \tag{19}$$

for functions f that depend both on angle θ and radius r, and

$$\|f\|^2_{L^2} = \int_{R_1}^{R_2} f(r)^2 r dr d\theta \tag{20}$$

$$\|f\|^2_{H^1} = \|f\|^2_{L^2} + \|f_r\|^2_{L^2} \tag{21}$$

for functions f only depending on the radius.

Remark 2: Lemma 1 (see the Appendix) shows that the L^2 and H^1 norms of τ can be written as a combination of the same norms of u and ζ. Hence, exponential stability in the L^2 norm (respectively, H^1 norm) of the origin for both ζ and u is equivalent to exponential stability of the origin in the L^2 norm (respectively, H^1 norm) of τ.

Thus, we study stability in the (v,u,ζ) system of (11)–(13). This system can be decomposed in two subsystem, the ζ subsystem with control law Υ, and the (v,u) subsystem with control laws V,U. Both subsystem are not coupled so we analyze and control them independently.

IV. Stabilization of ζ Subsystem

For Υ we set the following output feedback law:

$$\Upsilon = -q_0 \zeta(R2,\theta) \tag{22}$$

where $q_0 = 1/2(R_2 - R_1)$. Then, we get the following stability property (see the Appendix for the proof).

Proposition 1: Consider (13) with boundary conditions (16) and control law (22). Then, the equilibrium $\zeta \equiv 0$ is exponentially stable in the H^1 norm, i.e., there exists $C_1, c_1 > 0$ s.t.

$$\|\zeta(t)\|_{H^1_\theta} \le C_1 \mathrm{e}^{-c_1 t} \|\zeta(0)\|_{H^1_\theta}. \tag{23}$$

V. Stabilization of (v,u) Subsystem

In dealing with the (v,u) subsystem we follow a similar strategy to [16], but also adding an observer for state estimation.

First, we eliminate the convective term v_r for (11) and u_r for (12). Define $\breve{v} = v\sqrt{r}$, $\breve{u} = u\sqrt{r}$. Then $\breve{v}$ and $\breve{u}$ verify

$$\epsilon \breve{v}_t = A_1 \breve{u} - \lambda(r)\breve{v} + \breve{v}_{rr} \tag{24}$$

$$\breve{u}_t = A_2 \breve{v} - \lambda(r)\breve{u} + \breve{u}_{rr} \tag{25}$$

and boundary conditions

$$\breve{v}(R_1) = 0, \quad \breve{v}(R_2) = \breve{V} \tag{26}$$

$$\breve{u}_r(R_1) = \frac{\breve{u}(R_1)}{2R_1}, \quad \breve{u}_r(R_2) = \breve{U} \tag{27}$$

where $\lambda(r) = 3/4r^2$, $\breve{V} = \sqrt{R_2}V$, $\breve{U} = \breve{u}(R_2)/2R_2 + \sqrt{R_2}U$. We drop checks in the sequel for simplicity.

A. Control Design

First we design full state feedback laws V and U. We assume that the parameter ϵ is small enough so we can use singular perturbation theory [10], [16].

1) Quasi-Steady-State: The first step is to compute the quasi-steady-state (QSS) by setting $\epsilon = 0$ in (24). Then, the QSS is the solution of the linear ODE

$$v_{rr} - \lambda(r)v + A_1 u(r) = 0 \tag{28}$$

with boundary conditions $v(R_1) = 0, v(R_2) = V$. The solution is

$$v = \int_{R_1}^{r} f(r,s)u(s)ds - g(r)\left(\int_{R_1}^{R_2} f(R_2,s)u(s)ds - V(r)\right) \tag{29}$$

where

$$f(r,s) = -\frac{A_1}{2}\frac{r^2 - s^2}{\sqrt{rs}} \tag{30}$$

$$g(r) = \frac{r^2 - R_1^2}{R_2^2 - R_1^2}\sqrt{\frac{R_2}{r}}. \tag{31}$$

The velocity control V appears inside (29). We use it to put the QSS in strict integral feedback (strict-feedback) form [11], i.e., $v(t,r)$ should not depend on any value of $u(t,\rho)$ with $\rho > r$. Hence, we eliminate the non-strict-feedback integral (the second term) of (29). The strict-feedback structure is necessary so we can use the backstepping method for strict-feedback parabolic PDE's [14]. For that, set

$$V = \int_{R_1}^{R_2} f(R_2,s)u(s)ds \tag{32}$$

then the QSS is

$$v = \int_{R_1}^{r} f(r,s)u(s)ds. \tag{33}$$

2) Reduced Model: The reduced model is obtained by plugging the QSS into (25). We get

$$u_t = u_{rr} - \lambda(r)u + A_2 \int_{R_1}^{r} f(r,s)u(s)ds \tag{34}$$

$$u_r(R_1) = \frac{u(R_1)}{2R_1}, \quad u_r(R_2) = U \tag{35}$$

a strict-feedback parabolic PIDE with reaction and integral terms. We apply backstepping [14] to map (34)–(35) into the target system

$$w_t = w_{rr} - \lambda(r)w \tag{36}$$

$$w_r(R_1) = \frac{w(R_1)}{2R_1}, w_r(R_2) = 0 \tag{37}$$

where the reaction term λ has been kept since it helps stability. The backstepping transformation is defined as follows:

$$w = u - \int_{R_1}^{r} k(r,s)u(s)ds \tag{38}$$

where the kernel $k(r,s)$ is found to verify the following hyperbolic partial integro-differential equation in the domain $\mathcal{T} = \{R_1 \le r \le s \le R_2\}$:

$$k_{rr} - k_{ss} = (\lambda(r) - \lambda(s))k(r,s) - A_2 f(r,s) + A_2 \int_s^r f(\sigma,s)k(r,\sigma)d\sigma \tag{39}$$

$$k(r,r) = 0, \quad k_s(r,R_1) = \frac{k(r,R_1)}{2R_1}. \tag{40}$$

This equation was shown to be well-posed in [16], where the following explicit approximate solution for k was found:

$$\begin{aligned} k \approx -\frac{A_1 A_2}{2}\Bigg[&\frac{1}{3}(s^3 + 3r^2 s - 4(rs)^{3/2}) \\ &-2R_1(r-s)^2 + \frac{5}{2}\sqrt{\pi}R_1^3 \mathrm{e}^{1+(r-s)/R_1} \\ &\times \left(\mathrm{erf}(1) - \mathrm{erf}\left(\sqrt{1+\frac{r-s}{R_1}}\right)\right) \\ &+\frac{5}{3}\sqrt{R_1^2 + R_1(r-s)}\left(5R_1^2 + 2R_1(r-s)\right) \\ &+R_1^3\left(3\mathrm{e}^{(r-s)/R_1} - \frac{34}{3}\right) - 8R_1^2(r-s)\Bigg]. \end{aligned} \tag{41}$$

Using the kernel k, the control law U is found to be

$$U = \int_{R_1}^{R_2} k_r(R_2,s)u(s)ds. \tag{42}$$

Backstepping theory guarantees that U stabilizes the reduced model, and it was shown in [16] that for sufficiently small ϵ, the control laws V and U keep stabilizing the system.

B. Observer Design

Since control laws (32) and (42) require knowledge of the full state of the system, we design an observer to estimate the state from the measurements $v_r(R_2)$ and $u(R_2)$. We postulate our observer as a copy of the plant with output injection of measurement error, as follows:

$$\epsilon\hat{v}_t = \hat{v}_{rr} - \lambda(r)\hat{v} + A_1\hat{u} \tag{43}$$

$$\hat{u}_t = \hat{u}_{rr} - \lambda(r)\hat{u} + A_2\hat{v} + p_1(r)\left(u(R_2) - \hat{u}(R_2)\right) + p_2(r)\left(v_r(R_2) - \hat{v}_r(R_2)\right) \tag{44}$$

$$\hat{v}(R_1) = 0, \quad \hat{v}(R_2) = V \tag{45}$$

$$\hat{u}_r(R_1) = \frac{\hat{u}(R_1)}{2R_1} \tag{46}$$

$$\hat{u}_r(R_2) = U - p_{10}\left(u(R_2) - \hat{u}(R_2)\right) \tag{47}$$

where hats denote estimated variables, and p_1, p_2, and p_{10} are output injection gains, to be found. Defining the observer error variables as $\tilde{v} = v - \hat{v}$, $\tilde{u} = u - \hat{u}$, the observer error equations are

$$\epsilon\tilde{v}_t = \tilde{v}_{rr} - \lambda(r)\tilde{v} + A_1\tilde{u} \tag{48}$$

$$\tilde{u}_t = \tilde{u}_{rr} - \lambda(r)\tilde{u} + A_2\tilde{v} - p_1(r)\tilde{u}(R_2) - p_2(r)\tilde{v}_r(R_2) \tag{49}$$

$$\tilde{v}(R_1) = \tilde{v}(R_2) = 0 \tag{50}$$

$$\tilde{u}_r(R_1) = \frac{\tilde{u}(R_1)}{2R_1}, \quad \tilde{u}_r(R_2) = p_{10}\tilde{u}(R_2). \tag{51}$$

As in Section V-A, we apply singular perturbation theory to design output injection gains p_1, p_2, and p_{10}.

1) Quasi-Steady-State: Setting $\epsilon = 0$ in (48), the QSS is the solution of

$$\tilde{v}_{rr} - \lambda(r)\tilde{v} + A_1\tilde{u} = 0 \tag{52}$$

with $\tilde{v}(R_1) = \tilde{v}(R_2) = 0$. The solution is

$$\tilde{v} = -\int_r^{R_2} f(r,s)\tilde{u}(s)ds + \int_{R_1}^{R_2} h(r,s)\tilde{u}(s)ds \tag{53}$$

where

$$h(r,s) = g(R_2 + R_1 - r)f(R_1,s). \tag{54}$$

Using the measurement $v_r(R_2)$ to write the solution, the QSS is

$$\tilde{v} = -\int_r^{R_2} f(r,s)\tilde{u}(s)ds + l(r)v_r(R_2) \tag{55}$$

where

$$l(r) = \frac{r^2 - R_2^2}{2\sqrt{R_2 r}}. \tag{56}$$

Note that we have written the QSS in terms of an "upper-triangular" rather than a strict-feedback ("lower-triangular") integral of the state $\tilde{u}$. This means that $\tilde{v}(t,r)$ only depends on values of $\tilde{u}(t,\rho)$ with $\rho \ge r$. This is necessary for applying the backstepping observer design method for collocated systems [15], which makes use of an upper-triangular transformation.

2) Reduced Model: Plugging (55) into (48) we get the reduced model for the observer error, which is

$$\tilde{u}_t = \tilde{u}_{rr} - \lambda(r)\tilde{u} - A_2\left(\int_r^{R_2} f(r,s)\tilde{u}(s)ds - l(r)v_r(R_2)\right) - p_1(r)\tilde{u}(R_2) - p_2(r)\tilde{v}_r(R_2). \tag{57}$$

Set $p_2(r) = A_2 l(r)$. Then

$$\tilde{u}_t = \tilde{u}_{rr} - \lambda(r)\tilde{u} - A_2\int_r^{R_2} f(r,s)\tilde{u}(s)ds - p_1(r)\tilde{u}(R_2) \tag{58}$$

is a parabolic PDE in u with an upper-triangular integral term, and boundary conditions

$$\tilde{u}_r(R_1) = \frac{\tilde{u}(R_1)}{2R_1}, \tilde{u}_r(R_2) = p_{10}\tilde{u}(R_2). \tag{59}$$

Following the backstepping observer design method [15], we apply an upper-triangular transformation

$$\tilde{u} = \tilde{w} - \int_r^{R_2} p(r,s)\tilde{w}(s)ds \tag{60}$$

where $\tilde{w}$ verifies

$$\tilde{w}_t = \tilde{w}_{rr} - \lambda(r)\tilde{w} \tag{61}$$

$$\tilde{w}_r(R_1) = \frac{\tilde{w}(R_1)}{2R_1}, \quad \tilde{w}_r(R_2) = 0. \tag{62}$$

The kernel $p(r,s)$ is found to verify the following equation in the domain $\mathcal{T}$:

$$\begin{aligned} p_{ss} - p_{rr} &= (\lambda(s) - \lambda(r))\, p + A_2 f(r,s) \\ &\quad - A_2 \int_r^s f(r,\sigma)p(\sigma,s)d\sigma \end{aligned} \tag{63}$$

$$p_r(R_1,s) = \frac{p(R_1,s)}{2R_1}, \quad p(r,r) = 0. \tag{64}$$

From the kernel p the output injection gains in (58) and (59) are found to be $p_1 = -p_r(r,R_2)$ and $p_{10} = 0$.

Defining $\check{s} = r$, $\check{r} = s$, and $\check{p}(\check{r},\check{s}) = p(r,s)$, the kernel $\check{p}$ verifies

$$\begin{aligned} \check{p}_{\check{r}\check{r}} - \check{p}_{ss} &= (\lambda(\check{r}) - \lambda(\check{s}))\, \check{p} + A_2 f(\check{s},\check{r}) \\ &\quad - A_2 \int_{\check{s}}^{\check{r}} f(\check{s},\sigma)\check{p}(\check{r},\sigma)d\sigma \end{aligned} \tag{65}$$

$$\check{p}_{\check{s}}(\check{r},R_1) = \frac{\check{p}(\check{r},R_1)}{2R_1}, \quad \check{p}(\check{r},\check{r}) = 0. \tag{66}$$

Since $f(r,s) = -f(s,r)$, (65)–(66) are the same as (39)–(40), verified by k. Hence, it follows that (65)–(66) is well-posed and $p(r,s) = k(s,r)$, so that $p_1(r) = -k_s(R_2,r)$. Equation (41) gives then an explicit expression for the output injection gain p_1.

C. Output Feedback Controller

Combining the results of Sections V-A and V-B, we get the following output feedback controller:

$$V = \int_{R_1}^{R_2} f(R_2,s)\hat{u}(s)ds \tag{67}$$

$$U = \int_{R_1}^{R_2} k_r(R_2,s)\hat{u}(s)ds \tag{68}$$

where the estimate $\hat{u}(r)$ is obtained from

$$\epsilon\hat{v}_t = \hat{v}_{rr} - \lambda(r)\hat{v} + A_1\hat{u} \tag{69}$$

$$\begin{aligned} \hat{u}_t &= \hat{u}_{rr} - \lambda(r)\hat{u} + A_2\hat{v} \\ &\quad - k_s(R_2,r)\left(u(R_2) - \hat{u}(R_2)\right) \\ &\quad + A_2 l(r)\left(v_r(R_2) - \hat{v}_r(R_2)\right) \end{aligned} \tag{70}$$

$$\hat{v}(R_1) = 0, \quad \hat{v}(R_2) = V \tag{71}$$

$$\hat{u}_r(R_1) = \frac{\hat{u}(R_1)}{2R_1}, \quad \hat{u}_r(R_2) = U. \tag{72}$$

The backstepping method [14], [15] guarantees that the output feedback control laws stabilize the reduced model (34), thus stabilizing the system when $\epsilon = 0$.

D. Singular Perturbation Analysis for Small ϵ

Assume that ϵ is small but nonzero. Since $u = \hat{u} + \tilde{u}$ and $v = \hat{v} + \tilde{v}$, we show stability of the (u,v) system by proving stability in the $(\hat{v},\tilde{v},\hat{u},\tilde{u})$ coordinates. We begin stating the following proposition regarding $(\tilde{v},\tilde{u})$ (see the Appendix for the proof).

Proposition 2: Consider (48)–(49) with boundary conditions (50)–(51). Then, there exists ϵ^* such that if $\epsilon \in (0,\epsilon^*)$, the equilibrium $\tilde{u} \equiv \tilde{v} \equiv 0$ is exponentially stable in the H^1 norm, i.e., there exists $C_2, c_2 > 0$ s.t.

$$\|\tilde{v}(t)\|_{H^1} + \|\tilde{u}(t)\|_{H^1} \leq C_2 \mathrm{e}^{-c_2 t}\left(\|\tilde{v}(0)\|_{H^1} + \|\tilde{u}(0)\|_{H^1}\right). \tag{73}$$

Now we study the $(\hat{v},\hat{u})$ subsystem, which verifies (43)–(44). Since $\tilde{v}_r(R_2)$ and $\tilde{u}(R_2)$ feed into (44), it is not possible to obtain stability for $(\hat{v},\hat{u})$ alone; rather, the whole $(\hat{v},\tilde{v},\hat{u},\tilde{u})$ subsystem has to be considered. We get the following result.

Proposition 3: Consider (43)–(44) and (48)–(49), with boundary conditions (45)–(47) and (50)–(51), and control laws (67)–(68). Then, there exists ϵ^* such that if $\epsilon \in (0,\epsilon^*)$, the equilibrium $\hat{u} \equiv \hat{v} \equiv \tilde{u} \equiv \tilde{v} \equiv 0$ is exponentially stable in the H^1 norm, i.e., there exists $C_3, c_3 > 0$ s.t.

$$\begin{aligned} &\|\hat{v}(t)\|_{H^1} + \|\hat{u}(t)\|_{H^1} + \|\tilde{v}(t)\|_{H^1} + \|\tilde{u}(t)\|_{H^1} \\ &\quad \leq C_3 \mathrm{e}^{-c_3 t}\left(\|\hat{v}(0)\|_{H^1} + \|\hat{u}(0)\|_{H^1}\right. \\ &\quad\quad \left. + \|\tilde{v}(0)\|_{H^1} + \|\tilde{u}(0)\|_{H^1}\right). \end{aligned} \tag{74}$$

We skip the proof of Proposition 3, since it follows exactly the same lines as the proof of Proposition 2 (see the Appendix); the $(\hat{v},\hat{u})$ system can be proven exponentially stable in the H^1 norm when $\tilde{v} \equiv \tilde{u} \equiv 0$. Since the $(\hat{v},\hat{u})$ system is driven by $\tilde{v}_r(R_2)$ and $\tilde{u}(R_2)$, using the estimates in the proof of Proposition 2 the whole system is shown to be exponentially stable.

VI. Main Result

Using the definition of Γ in terms of U and Υ, and writing the observer equations in terms of the original measurements $v_r(R_2)$ and $\tau(R_2,\theta)$, we get the output feedback control laws for the entire system

$$V = \int_{R_1}^{R_2} \frac{f(R_2,s)}{\sqrt{R_2}}\hat{u}(s)ds \tag{75}$$

$$\begin{aligned} \Gamma &= \frac{1}{\pi}\left(q_0 + \frac{1}{2\sqrt{R_2^3}}\right)\int_0^{2\pi} \tau(t,R_2,\theta)\cos\theta d\theta \\ &\quad - q_0\tau(t,R_2,\theta) + \int_{R_1}^{R_2} \frac{k_r(R_2,s)}{\sqrt{R_2}}\hat{u}(s)ds \end{aligned} \tag{76}$$

where

$$\epsilon\hat{v}_t = \hat{v}_{rr} - \lambda(r)\hat{v} + A_1\hat{u} \tag{77}$$

$$\hat{u}_t = \hat{u}_{rr} - \lambda(r)\hat{u} + A_2\hat{v} - k_s(R_2,r) \times \left(\frac{\sqrt{R_2}}{\pi}\int_0^{2\pi}\tau(t,R_2,\theta)\cos\theta d\theta - \hat{u}(R_2)\right) + A_2 l(r)\left(\sqrt{R_2}v_r(R_2) - \hat{v}_r(R_2)\right) \tag{78}$$

$$\hat{v}(R_1) = 0, \hat{v}(R_2) = \sqrt{R_2}V \tag{79}$$

$$\hat{u}_r(R_1) = \frac{\hat{u}(R_1)}{2R_1} \tag{80}$$

$$\hat{u}_r(R_2) = \int_{R_1}^{R_2} k_r(R_2,s)\hat{u}(s)ds. \tag{81}$$

From Propositions 1 and 3, Lemma 1 and Remark 2, we get the following result.

Theorem 1: Consider system (7)–(8) with boundary conditions (3)–(6) and output feedback control laws (75)–(81). Then, there exists $\epsilon^* > 0$ such that for $\epsilon \in (0, \epsilon^*)$, the equilibrium $v \equiv \tau \equiv \tilde{v} \equiv \tilde{u} \equiv 0$ is exponentially stable in the H^1 norm, i.e., there exists $C_4, c_4 > 0$ s.t.

$$\|v(t)\|_{H^1} + \|\tau(t)\|_{H^1_\theta} + \|\tilde{v}(t)\|_{H^1} + \|\tilde{u}(t)\|_{H^1} \le C_4 e^{-c_4 t}\left(\|v(0)\|_{H^1} + \|\tau(0)\|_{H^1_\theta} + \|\tilde{v}(0)\|_{H^1} + \|\tilde{u}(0)\|_{H^1}\right). \tag{82}$$

VII. Simulation Study

We use for simulation the same prototypical case that was shown open-loop unstable in [16]. Numerical computations are carried out using a spectral method (using Fourier series) combined with the Crank–Nicholson method. The parameters of the system had the following numerical values: $R_1 = 1.1975$ ft, $R_2 = 1.2959$ ft, $P = 8.06$, $Ra = 50$, $C = 7.8962 \times 10^3$. For these values, it is shown in [16] that the kernel approximation given by (41) is very good.

In Fig. 3, we show the shape of the kernels appearing in our control law. Note that the temperature control kernel $k_r(R_2, s)$ gives more weight in the control law to information near the inner boundary—as the boundary controller is on the opposite side, it has to react more aggressively to compensate fluctuations of temperature in the interior part of the domain. This is also true for the velocity control kernel $f(R_2, r)$ and velocity output injection gain $l(r)$ (which is not explicitly shown as $l(r) = f(R_2, r)/A_1$). The temperature output injection gain $k_s(R_2, s)$ is larger in the middle of the loop, where the states are somewhat more difficult to estimate (near the boundaries some information is known *a priori*).

In Fig. 4, closed-loop simulations of the plant show how the states converge exponentially towards the equilibrium profile fairly quickly. We also plot the observer error, that converges to zero. In Fig. 5, we show the magnitude of the control law Γ.

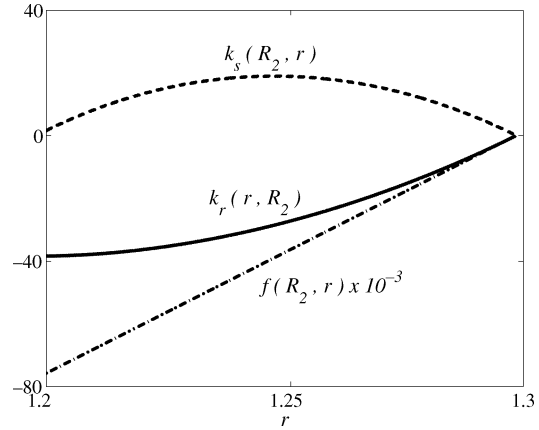

Fig. 3. Control kernel $k_r(R_2, r)$ (solid line), observer output injection kernel $k_s(R_2, r)$ (dashed line), and velocity control kernel $f(R_2, r)$ (dashed-dotted line).

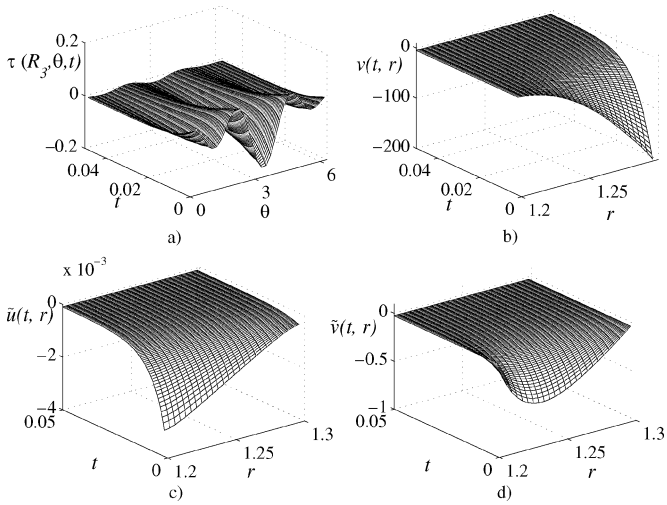

Fig. 4. Closed-loop simulation. a) Temperature perturbation $\tau(t, r, \theta)$ at radius $R_3 = (R_1 + R_2)/2$. b) Velocity $v(t, r)$. c) Observer error $\tilde{u}(t, r)$. d) Observer error $\tilde{v}(t, r)$.

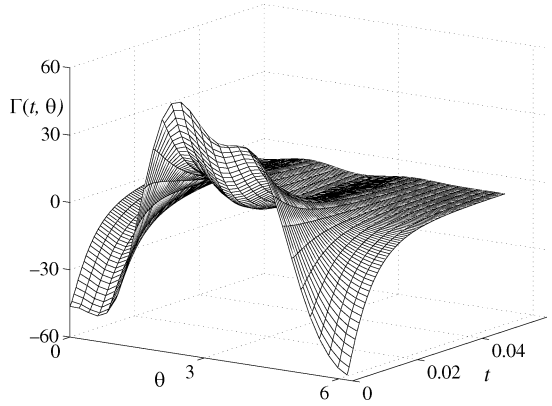

Fig. 5. Magnitude of temperature control law Γ.

VIII. Conclusion

A combination of singular perturbation theory and backstepping for parabolic PDEs has been successfully employed to stabilize a thermal fluid confined in a convection loop which is open-loop unstable. Our design, based on the singular perturbation assumption of a large enough Prandtl number—which is true for many fluids—makes the plant closed-loop stable. Our controller uses rotation and heat flux actuation at the outer

boundary, and needs measurements of temperature and skin friction only at the same boundary. Control and observer gains are found using a backstepping design procedure, which is both conceptually and computationally simple, requiring only to solve a hyperbolic linear equation for obtaining the control law; an accurate closed-form approximation is provided. A simulation study for the fully nonlinear plant is also provided.

The case that the Prandtl number is small, rather than large, is also of physical interest. In that case, temperature becomes the fast variable while velocity is now the slow variable. Our design strategy is still valid just interchanging the role of velocity and temperature in the control design.

Other possible extensions include considering more complex geometries, for instance infinite 3-D channel flow between two parallel plates, where the upper plate is cooled and the lower plate is heated. For large enough heat flux at the boundaries, a Rayleigh–Bernard type of convective instability develops. This flow is used as a benchmark for turbulence study, as it is known to become unstable and transition to a turbulent regime for large Reynolds numbers; thus, adding a convective instability makes the problem even more challenging. Since it is possible to stabilize the velocity field—without temperature gradients—using backstepping [7], we expect that the system with convection can be stabilized using a similar approach to this paper. Actuation of velocity and heat flux at the boundaries will be necessary, as well as measurements of temperature and skin friction at one of the walls.

Our current approach requires linearizing the plant as a first step. This is a requirement of the linear backstepping design method, and it is a natural extension to consider instead the very challenging problem of stabilizing the fully nonlinear plant. Nonlinear backstepping theory for infinite dimensional system [17] is a new theory under development that provides a design method to stabilize a class of nonlinear PDEs with nonlinearities given in the form of a Volterra series. This method might be applicable as this problem falls in the class after applying singular perturbations, due to the bilinear structure of the nonlinearity (it is well known [13] that the solution of a bilinear equation is in the form of a Volterra series).

APPENDIX

In the Appendix we prove some technical results that were used in this paper.

Lemma 1: For u and ζ defined as in Section III, we have that

$$||\tau||^2_{L^2_\theta} = \pi||u||^2_{L^2} + ||\zeta||^2_{L^2_\theta} \tag{83}$$

$$||\tau||^2_{H^1_\theta} = \pi||u||^2_{H^1} + \pi\int_{R_1}^{R_2}\frac{u^2(t,r)}{r^2}rdr + ||\zeta||^2_{H^1_\theta} \tag{84}$$

and the $||\tau||_{H^1_\theta}$ norm is equivalent to the norm

$$||u||_{H^1} + ||\zeta||_{H^1_\theta}. \tag{85}$$

Proof: Using (17), we get

$$\begin{aligned}
&\int_0^{2\pi}\int_{R_1}^{R_2}\tau^2 rdrd\theta \\
&\quad = \pi\int_{R_1}^{R_2}u^2(t,r)rdr + \int_0^{2\pi}\int_{R_1}^{R_2}\zeta^2 rdrd\theta \\
&\qquad + \int_{R_1}^{R_2}u(t,r)\left(\int_0^{2\pi}\zeta\cos\theta d\theta\right)rdr \\
&\quad = \pi\int_{R_1}^{R_2}u^2(t,r)rdr + \int_0^{2\pi}\int_{R_1}^{R_2}\zeta^2 rdrd\theta
\end{aligned} \tag{86}$$

so (83) follows. Similarly, we have that

$$\begin{aligned}
&\int_0^{2\pi}\int_{R_1}^{R_2}\tau_r^2 rdrd\theta \\
&\quad = \pi\int_{R_1}^{R_2}u_r^2(t,r)rdr + \int_0^{2\pi}\int_{R_1}^{R_2}\zeta_r^2 rdrd\theta \\
&\qquad + \int_{R_1}^{R_2}u_r(t,r)\left(\int_0^{2\pi}\zeta_r\cos\theta d\theta\right)rdr \\
&\quad = \pi\int_{R_1}^{R_2}u_r^2(t,r)rdr + \int_0^{2\pi}\int_{R_1}^{R_2}\zeta_r^2 rdrd\theta
\end{aligned} \tag{87}$$

and we also have that

$$\begin{aligned}
&\int_0^{2\pi}\int_{R_1}^{R_2}\frac{\tau_\theta^2}{r^2}rdrd\theta \\
&\quad = \pi\int_{R_1}^{R_2}\frac{u^2(t,r)}{r^2}rdr + \int_0^{2\pi}\int_{R_1}^{R_2}\frac{\zeta_\theta^2}{r^2}rdrd\theta \\
&\qquad - \int_{R_1}^{R_2}u(t,r)\left(\int_0^{2\pi}\zeta_\theta\sin\theta d\theta\right)rdr \\
&\quad = \pi\int_{R_1}^{R_2}\frac{u^2(t,r)}{r^2}rdr + \int_0^{2\pi}\int_{R_1}^{R_2}\frac{\zeta_\theta^2}{r^2}rdrd\theta \\
&\qquad + \int_{R_1}^{R_2}u(t,r)\left(\int_0^{2\pi}\zeta\cos\theta d\theta\right)rdr \\
&\quad = \pi\int_{R_1}^{R_2}u_r^2(t,r)rdr + \int_0^{2\pi}\int_{R_1}^{R_2}\zeta_r^2 rdrd\theta
\end{aligned} \tag{88}$$

so (84) follows. The norm equivalence follows from (84) and Poincare's inequality for u. ■

Proof of Proposition 1: Define

$$\begin{aligned}
L = &\frac{1}{2}\int_0^{2\pi}\int_{R_1}^{R_2}\left(\frac{\zeta_\theta^2(r,\theta)}{r^2} + \zeta_r^2(r,\theta) + \zeta^2(r,\theta)\right)rd\theta dr \\
&+ \frac{q_0R_2}{2}\int_0^{2\pi}\zeta^2(R_2,\theta)d\theta
\end{aligned} \tag{89}$$

then

$$\begin{aligned}
\frac{dL}{dt} = &-\int_0^{2\pi}\int_{R_1}^{R_2}\left(\frac{\zeta_{\theta\theta}}{r^2} + \zeta_{rr} + \frac{\zeta_r}{r}\right)^2 rd\theta dr \\
&-\int_0^{2\pi}\int_{R_1}^{R_2}\left(\frac{\zeta_\theta^2}{r^2} + \zeta_r^2\right)rd\theta dr \\
&+\int_0^{2\pi}R_2\zeta_r(R_2,\theta)\zeta(R_2,\theta)d\theta \\
\le &-DL
\end{aligned} \tag{90}$$

for some $D > 0$, where we have used (22), Poincare's inequality (see the appendix of [16]) and the fact that $R_2 - R_1 < 1$. As L is equivalent to the H^1_θ norm of ζ, H^1 exponential stability follows. ∎

Proof of Proposition 2: Define $\tilde{z} = \tilde{v} - \tilde{v}_{ss}$, where

$$\tilde{v}_{ss} = -\int_r^{R_2} f(r,s)\tilde{u}(\xi)d\xi + \int_{R_1}^{R_2} h(r,s)\tilde{u}(\xi)d\xi \tag{91}$$

and define $\tilde{w}$ by the backstepping transformation (60). From $(\tilde{z}, \tilde{w})$ definitions and the fact that the kernel of the transformation is $\mathcal{C}^2$, exponential stability in $(\tilde{z}, \tilde{w})$ coordinates implies exponential stability for $(\tilde{v}, \tilde{u})$. The observer error plant in $(\tilde{z}, \tilde{w})$ coordinates is

$$\epsilon\tilde{z}_t = \tilde{z}_{rr} - \lambda(r)\tilde{z} - \epsilon(\tilde{v}_{ss})_t \tag{92}$$

$$\tilde{w}_t = \tilde{w}_{rr} - \lambda(r)\tilde{w} + A_2\tilde{z} - A_2 l_2(r)\tilde{z}_r(R_2) \tag{93}$$

$$\tilde{z}(R_1) = \tilde{z}(R_2) = 0 \tag{94}$$

$$\tilde{w}_r(R_1) = \frac{\tilde{w}(R_1)}{2R_1}, \tilde{w}_r(R_2) = 0. \tag{95}$$

In (92), we need to express $(\tilde{v}_{ss})_t$ in terms of z and w. First, we write

$$\tilde{v}_{ss} = \int_r^{R_2} \tilde{f}(r,s)\tilde{w}(s)ds + \int_{R_1}^{R_2} \tilde{h}(r,s)\tilde{w}(s)ds \tag{96}$$

where

$$\tilde{f}(r,s) = -f(r,s) + \int_r^{R_2} f(r,\sigma)p(\sigma,s)d\sigma \tag{97}$$

$$\tilde{h}(r,s) = h(r,s) - \int_{R_1}^{R_2} h(r,\sigma)p(\sigma,s)d\sigma. \tag{98}$$

Then, using (93)

$$\begin{aligned}(\tilde{v}_{ss})_t = &\int_r^{R_2} \left(\tilde{f}_{ss}(r,s) - \tilde{f}(r,s)\lambda(s)\right) w(s)ds \\ &+ \int_{R_1}^{R_2} \left(\tilde{h}_{ss}(r,s) - \tilde{h}(r,s)\lambda(s)\right) w(s)ds \\ &- (\tilde{f}_s(r,R_2) + \tilde{h}_s(r,R_2))w(R_2) - A_2 z_r(R_2) \\ &\times \left(\int_r^{R_2} \tilde{f}(r,s)l_2(s)ds + \int_{R_1}^{R_2} \tilde{h}(r,s)l_2(s)ds\right) \\ &+ \left(\tilde{h}_s(r,R_1) - q\tilde{h}(r,R_1)\right) w(R_1) + \tilde{f}_s(r,r)w(r) \\ &+ A_2\int_r^{R_2} \tilde{f}(r,s)z(s)ds + A_2\int_{R_1}^{R_2} \tilde{h}(r,s)z(s)ds.\end{aligned} \tag{99}$$

Define the Lyapunov functions

$$L_1 = \frac{1}{2}\int_{R_1}^{R_2} \left(\tilde{z}_r^2 + 3\frac{\tilde{z}^2}{R_1^2}\right) dr \tag{100}$$

$$L_2 = \frac{1}{2}\int_{R_1}^{R_2} \left(\tilde{w}_r^2 + 3\frac{\tilde{w}^2}{R_1^2}\right) dr + \frac{\tilde{w}(R_1)^2}{4R_1} \tag{101}$$

which are equivalent, using Poincare's inequality, to the H^1 norms of $\tilde{z}$ and $\tilde{w}$, respectively. Then

$$\begin{aligned}\frac{dL_1}{dt} = &-\frac{1}{\epsilon}\int_{R_1}^{R_2} \left(\hat{z}_{rr}^2 + \left(\lambda + \frac{3}{R_1^2}\right)\hat{z}_r^2 + 3\frac{\lambda\hat{z}^2}{R_1^2}\right) dr \\ &+ \frac{1}{\epsilon}\int_{R_1}^{R_2} \frac{\lambda''(r)}{2}\hat{z}^2 dr \\ &+ \int_{R_1}^{R_2} \left(-\hat{z}_{rr} + 3\frac{\hat{z}}{R_1^2}\right)(\tilde{v}_{ss})_t dr \\ \le &-\frac{D_1}{\epsilon}\int_{R_1}^{R_2} \left(\hat{z}_{rr}^2 + \hat{z}_r^2 + 3\frac{\hat{z}^2}{R_1^2}\right) dr \\ &+ D_2\int_{R_1}^{R_2} \left(\hat{z}_{rr}^2 + \hat{z}_r^2 + w_r^2 + w^2\right) dr\end{aligned} \tag{102}$$

where D_1 and D_2 are positive, and where we have used that $\lambda''(r) \le 3\lambda(r)/R_1^2$, and Poincare's and Young's inequality to bound all the terms from $(v_{ss})_t$. Similarly

$$\begin{aligned}\frac{dL_2}{dt} = &-\int_{R_1}^{R_2} \left(\hat{w}_{rr}^2 + \left(\lambda + \frac{3}{R_1^2}\right)\hat{w}_r^2 + 3\frac{\lambda\hat{w}^2}{R_1^2}\right) dr \\ &+ \int_{R_1}^{R_2} \frac{\lambda''(r)}{2}\hat{w}^2 dr + \frac{\hat{w}(R_1)\hat{w}_t(R_1)}{2R_1} \\ &- \hat{w}_r(R_1)\hat{w}_t(R_1) - \left(\lambda(R_1) + \frac{3}{R_1^2}\right) \\ &\times \hat{w}_r(R_1)\hat{w}(R_1) + \frac{\lambda'(R_1)}{2}\hat{w}(R_1)^2 \\ &+ \int_{R_1}^{R_2} \left(-\hat{w}_{rr} + 3\frac{\hat{w}}{R_1^2}\right) \times A_2\left(\tilde{z} - l_2(r)\tilde{z}_r(R_2)\right) dr \\ \le &-D_3\left(\int_{R_1}^{R_2} \left(\hat{w}_{rr}^2 + \hat{w}_r^2 + 3\frac{\tilde{w}^2}{R_1^2}\right) dr \right. \\ &\left. + \frac{\hat{w}(R_1)^2}{4R_1}\right) + D_4\int_{R_1}^{R_2} \left(\hat{z}_{rr}^2 + \hat{z}_r^2\right) dr.\end{aligned} \tag{103}$$

Setting $L_3 = L_1 + D_5 L_2$, and using Poincare's inequality, it follows that for some positive (and possibly large) D_5, there exists ϵ^* such that for $\epsilon \in (0, \epsilon^*)$, one has that

$$\frac{dL_3}{dt} \le -D_6 L_3 \tag{104}$$

from where exponential stability is obtained. ∎

REFERENCES

[1] O. M. Aamo, A. Smyshlyaev, and M. Krstic, "Boundary control of the linearized Ginzburg-Landau model of vortex shedding," *SIAM J. Control Opt.*, vol. 43, pp. 1953–1971, 2005.

[2] M.-R. Alam, W.-J. Liu, and G. Haller, "Closed-loop separation control: An analytic approach," *Phys. Fluids*, vol. 18, p. 043601, 2006.

[3] J. Baker, A. Armaou, and P. D. Christofides, "Nonlinear control of incompressible fluid flow: Application to Burgers' equation and 2D channel flow," *J. Math. Anal. Appl.*, vol. 252, pp. 230–255, 2000.

[4] T. R. Bewley, "Flow control: New challenges for a new Renaissance," *Progress Aerosp. Sci.*, vol. 37, pp. 21–58, 2001.

[5] D. Boskovic and M. Krstic, "Nonlinear stabilization of a thermal convection loop by state feedback," *Automatica*, vol. 37, pp. 2033–2040, 2001.

[6] J. A. Burns, B. B. King, and D. Rubio, "Feedback control of a thermal fluid using state estimation," *Int. J. Computational Fluid Dyn.*, vol. 11, pp. 93–112, 1998.
[7] J. Cochran, R. Vazquez, and M. Krstic, "Backstepping boundary control of Navier-Stokes channel flow: A 3D extension," presented at the 25th Amer. Control Conf. (ACC), Minneapolis, MN, 2006.
[8] M. Hogberg, T. R. Bewley, and D. S. Henningson, "Linear feedback control and estimation of transition in plane channel flow," *J. Fluid Mechan.*, vol. 481, pp. 149–175, 2003.
[9] P. G. Drazin, *Introduction to Hydrodynamic Stability*. Cambridge, U.K.: Cambridge University Press, 2002.
[10] P. V. Kokotovic, H. K. Khalil, and J. O'Reilly, *Singular Perturbation Methods in Control*. Philadelphia, PA: SIAM, 1999, Classics in Applied Mathematics.
[11] M. Krstic, I. Kanellakopoulos, and P. V. Kokotovic, *Nonlinear and Adaptive Control Design*. New York: Wiley, 1995.
[12] B. Protas and A. Styczek, "Optimal control of the cylinder wake in the laminar regime," *Phys. Fluids*, vol. 14, no. 7, pp. 2073–2087, 2002.
[13] W. J. Rugh, "Nonlinear system theory: The Volterra/Wiener approach," 1981. [Online]. Available: http://www.ece.jhu.edu/rugh/volterra/book.pdf
[14] A. Smyshlyaev and M. Krstic, "Closed form boundary state feedbacks for a class of partial integro-differential equations," *IEEE Trans. Autom. Control*, vol. 49, no. 12, pp. 2185–2202, Dec. 2004.
[15] A. Smyshlyaev and M. Krstic, "Backstepping observers for parabolic PDEs," *Syst. Control Lett.*, vol. 54, pp. 1953–1971, 2005.
[16] R. Vazquez and M. Krstic, "Explicit integral operator feedback for local stabilization of nonlinear thermal convection loop PDEs," *Syst. Control Lett.*, vol. 55, pp. 624–632, 2006.
[17] R. Vazquez and M. Krstic, "Control of 1-D parabolic PDEs with Volterra nonlinearities Part I: Design," *Automatica*, vol. 44, pp. 2778–2790, 2008.
[18] R. Vazquez and M. Krstic, "A closed-form feedback controller for stabilization of linearized Navier-Stokes equations: The 2D Poiseuille flow," *IEEE Trans. Autom. Control*, vol. 52, no. 12, pp. 2298–2312, Dec. 2007.
[19] R. Vazquez, E. Schuster, and M. Krstic, "Magnetohydrodynamic state estimation with boundary sensors," *Automatica*, vol. 44, pp. 2517–2527, 2008.

Rafael Vazquez (S'05–M'08) received the B.S. degrees in electrical engineering and mathematics from the University of Seville, Seville, Spain, and the Ph.D. and M.S. degrees in aerospace engineering from the University of California, San Diego.

He is an Assistant Professor with the Aerospace and Fluid Mechanics Department, University of Seville. He is a coauthor of the book *Control of Turbulent and Magnetohydrodynamic Channel Flows* (Birkhauser, 2007). He was a CTS Marie Curie Fellow at the Université Paris-Sud (2005). His research interests include nonlinear control, control of distributed parameter systems, dynamical systems, and applications to flow control, orbital mechanics, air traffic control and nanomechatronics.

Dr. Vazquez was a finalist for the Best Student Paper Award in the 2005 CDC.

Miroslav Krstic (S'92–M'95–SM'99–F'02) is the Sorenson Distinguished Professor and the founding Director of the Cymer Center for Control Systems and Dynamics, University of California, San Diego. He is a coauthor of the books *Nonlinear and Adaptive Control Design* (Wiley, 1995), *Stabilization of Nonlinear Uncertain Systems* (Springer-Verlag, 1998), *Flow Control by Feedback* (Springer-Verlag, 2002), *Real-time Optimization by Extremum Seeking Control* (Wiley, 2003), *Control of Turbulent and Magnetohydrodynamic Channel Flows* (Birkhauser, 2007), and *Boundary Control of PDEs: A Course on Backstepping Designs* (SIAM, 2008).

Dr. Krstic was a recipient of the Axelby and Schuck Paper Prizes, NSF Career, ONR Young Investigator, and PECASE Awards, the UCSD Research Award. He is a Fellow of IFAC and has held the appointment of Springer Distinguished Professor of Mechanical Engineering at University of California, Berkeley. His editorial service includes IEEE TRANSACTIONS ON AUTOMATIC CONTROL, *Automatica*, *SCL*, and *International Journal of Adaptive Control and Signal Processing*. He was VP Technical Activities and Chair of the Fellow Evaluation Committee of IEEE Control Systems Society.